Challenges of the Promise of Internet of Things (IoT) in Multi-Hop Communication Systems

Chowdhury Sajadul Islam [1], Mohammad Sarwar Hossain Mollah [2]

[1] *Department of Computer Science & Engineering*, Uttara University, Dhaka, Bangladesh.
[2] *Department of CIS*, Daffodil International University, Dhaka, Bangladesh.

chowdhury.iub@gmail.com, headcis@daffodilvarsity.edu.bd

***Abstract* - This paper centers around solutions for the Internet of Things (IoT) challenges in multi-hop connections and the execution of a physical layer network coding (PNC) model for relay broadcasts. For multi-hop transmission, PNC is contemplated as a vigorous solution for multi-hop packet transaction in the linear network topology. The PNC usage has numerous troubles, almost remarkably Carrier-Frequency Offsets (CFO) and timing synchronization. Within the Multiple Access (MA) phase, the relay has to acquire a signal from 2 sources, tracking the CFOs from 2 transmitters when their signals are applied to one of the principal complications. Focusing on practical and implementation concerns of PNC systems, various challenges have been covered and a Software Defined Radio (SDR); PNC technology established on Universal Software Radio Peripheral (USRP) techniques are proposed and applied. Afterward, big computer simulation and experimental outcomes are depicted to evaluate the operation of the urged algorithms in contrast with presently applied technology.**

Keywords - IoT; Multiple Access; Network Coding; GNURadio; Frequency Offsets

I. INTRODUCTION

The implication of IoT can never be comprehended without of sensors. Sensor systems (*SS*) applied as a part of assuring and metering applications are one of the key and first usages of IoT. One of the progressions that are predicting for multi-hop sensor network usage is physical layer (*layer*-1) network coding. It can enhance the end-to-end output by minimizing the amount of time slots that are required for a multi-hop communicating while confirming an acceptable untruth rate. Implementing a solution for execution troubles of *PNC*, the chance of a real-life *PNC* process is depicted by a *SDR* execution on *GNURadio* platform. Typical enforcement arguments are then including in both simulation and analytic thinking. A probable PNC execution has multiple experiments, various clearly timing synchronization and *CFO*. In the Multiple Access (*MA*) phase, the relay has to receive a signal from two sources, pursuing the *CFOs* from 2 transmitters while their signals are overlying is one of the primary obstacles. Present executions require an intervention free part into every signal which seems with a high overhead and is excessive for multi-hop scenarios.

II. BACKGROUND

Multi-hop transmission has always been unmanageable for wireless networks signaling system because of the mutual interference. While the amount of hops arises, the point to point throughput permits significantly. A famous research work has been applied to get the output and authenticity of multi-hop transmissions. Detecting collision as the primary barrier to multi-hop transmission, various new technologies have come out. Technologies e.g. straight interruption cancelation [1], multi-packet detection and collision resolution applying zigzag [2], interruption system [3, 4], and full-duplex (*FD*) transmissions [5] have all tested to address interruption and broadcast case of wireless channel in their favor. Another recommending technology is *PNC* [6]. It can perform a robust result for multi-hop communication systems.

III. ISSUES OF IMPLEMENTATION

We made physical layer network coding on *GNURadio* and *USRP* to build the multi-hop wireless testbed. For *MPNC*, the receiver and transmitter in a single-hop communication can be made applying regular transmitting and receiving chains [6,7]. In our paper, conventional Binary Phase Shift Keying (*BPSK*) blocks of *GNURadio* are applied for all stairs of transmission, modulation, timing retrieval, phase tracking and demodulation. For *MA* transmissions, beacons from 2 transmitters are synchronized in the stages of symbol. The synchronization result has been step by step observed, e.g., Source-Sync [7] can acquire low-overhead spread synchronization with the efficiency apartment of 10*ns*, fewer than the symbol length (e.g., 802.11 *OFDM* symbol duration are 4 μs). In outside scenarios synchronization of packets can be arrived by the exercise of *GPS* receivers. Besides, by intends of OFDM technology can cover the symbol period of time and produce the symbol level synchronization easier [8]. It is worth citing that the exactness of required synchronization depends upon the importance of symbol length. The simply requirement is

that the synchronization fault is little in measured with symbols gap. So long as the nodes are synchronized, the assumption of having an equivalent length among all transmitters to the relay can be reduced by computing the propagation time divergence and offset it when the transmissions are began. As synchronization for an attached *TDMA* network is relatively simple and it in point of fact creates the estimate and compensation of *CFO*s and detection of preamble by the *MA* transmission more complicated, we apply a *MIMO* line to synchronize the transmitters in our *USRP* testbed, and center on the most tricky piece, the receiver of *MA* communication with symbol-level synchronization.

A. Formulation of Signal forImplementation

Afterward the oscillator at the mixer of practical devices is never fixed; the live carrier frequency of accurate device may be somewhat changed from the supposed importance. This builds a little rotating level to continue in the signal afterwards the mixer. In standard point-to-point transmissions, this frequency offset can be determined and compensated applying state tracking algorithms. The related algorithms are no more useful in *MA* transmissions as the signals are from 2 sources and there are 2 frequency offsets, so the final state cannot be took out by a plain multiplication. Various algorithms have been suggested [8, 9, 10, 11] to neutralize the affect of CFO when a diversity of signals are combined at the receiver. These algorithms each required a little portion of the congestion-free region in 2 signals, which are not instantly relevant for MPNC with symbol level synchronization. Some other methods is to apply the mean of 2 frequency offsets to partly repair the frequency offsets for *PNC*-*MA* transmission [8]. In multi-hop scenes, fault distribution is a severe obstacle than that in the 2-hop PNC instance, so an exact cause that can absolutely compensate 2-CFOs is required. Regarding that nodes *U* and *V* are transferring symbol u_k and r_k at the k_{th} symbol interval, severally, the baseband signal can be defined as:

$$x(t)=\sum_{k=0}^{k=N} u_k g(t-kT), \qquad \text{and} \tag{1}$$

$$y(t)=\sum_{k=0}^{k=N} v_k g(t-kT), \tag{2}$$

correspondingly, where g(t) denoted the pulse for the pulse shaping step (a root raised cosine (RRC) pulse is applied here), N is the number of symbols in a packet, and T is the interval of symbol. Providing the received signal while:

$$r(t)=x(t-\tau)\mathrm{H}_u e^{j2\pi(f_u)t}+\mathrm{y}(t-\tau)\mathrm{H}_v e^{j2\pi(f_v)t}, \tag{3}$$

where f_u (f_v) is the CFOs referring the oscillator of the receiver and that of *U(V)*, correspondingly, and τ is the delay-time. In the *MA* transmission, f_u and f_v can be guessed at the starting of each packet. Regarding the wireless carriers to be frequency straight and stationary throughout the latency of a packet, H_u (H_v) can be determined with one tap, basically a complex number. The obtained signal afterwards the Analog to Digital Converter (*ADC*) is defined by:

$$r_n = h_1\, \mathrm{x} e^{j\omega_1 n+\phi_1} + h_2\, \mathrm{y} e^{j\omega_2 n+\phi_2}, \tag{4}$$

where h_i, are the achieves states and digital frequency offsets enforced by the channel and the receiver circuit, correspondingly.

B. Retrieval of Timing

Contingent upon the sampling rate of the Digital to Analog Converter (*DAC*), every symbol is represented by a fixed amount of samples. This parameter is defined Samples per Symbol (*SpS*) and can be detected as Tf_s, where f_s is the example rate of the DAC. In the wake of passing the obtained signal from the coordinated filter, the later stage is to down sample the signal to 1 sample per symbol before detection. In the digital domain, depending upon the match between the transmitter and receiver's clocks, just one of the samples alternatively of a symbol is applied for detection and the space between authorized samples is equal to *SpS*. As depicted in Fig.1 to obtain the legal sample, the signal is separated into varied branches and demolished with various time delays, from 0 to *SpS* 1. The signal after down-sampling can be showed as:

$$s_k = h_1 u_k\, e^{j(SpS)\omega_1 n+\phi_1} + h_2 v_k\, e^{j(SpS)\omega_2 n+\phi_2} \tag{5}$$

Each branch is then applied for preamble detection intentions and the outcome is attached to a change the similar preamble detection algorithm is ran for all branches. If a preamble is detected, the signal would be annotated with a tag consisting of ϕ_i and ω_i (i= *1, 2*). The switch then copies only the branch with a tag to output. It is probably to detect a preamble in more than a single branch. The preamble sensor block also attached the average square error of detecting so the switch can select the branch with the finest signal to noise ratio (*SNR*).

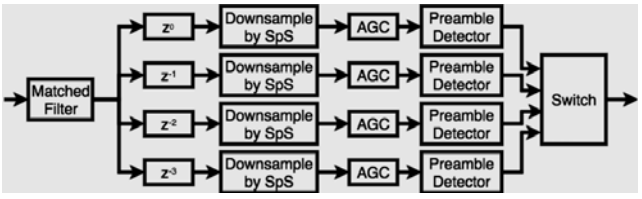

Fig. 1. Chain model of receiver.

C. CFO Estimater and MA Receiver

To assist the receiver guess *CFOs* and detect *MA* transmissions, each frame begins with a *Sync* preamble and a start of frame delimiter (*SFD*) component. The sync preamble is a sequence of 0s and 1s, and the *SFD* is wont to affirm the detection of a packet. In this paper, the Sync preambles for node *U* and *V* are "1010...10" and "0101...01", correspondingly, which is alike to the packet construction used in the IEEE 802.11 *FH-PHY*. Before utilizing the signal to detect a preamble, the signal is coming from an Automatic Gain Control (*AGC*) unit, in order that steady the channel gains, h_1 and h_2. In a window with a large amount of symbols, there exists at the least one instant that symbols from both roots has an equal or very near state and have been surplus constructively. Hence the *AGC* sets the max supreme measure of symbols to 2. For *BPSK*, *+1* and *-1* signifies *1* and *0*, sequentially. If we indicator all symbols of the *sync* portion beginning from 0, the k_{th} obtained symbols of Sync preamble can be denoted as:

$$s_k = (-1)^{k+1} e^{p_{1,k}} - (-1)^k \, \mathrm{e}^{p_{2},k}, \tag{6}$$

for stability, we switch all odd indexed symbols of Sync with their opposite so the k_{th} symbol can be defined as:

$$s'_k = e^{p_{1,k}} - \mathrm{e}^{p_{2},k}. \tag{7}$$

There are 2 states of $p_{1,k}$ and $p_{2,k}$ can be defined by solving the Eq. 8 as follows:

$$\begin{cases} \mathrm{Re}(s'_k) = \cos(p_{1,\mathrm{k}}) - \cos(p_{2,\mathrm{k}}), \\ \mathrm{Im}(s'_k) = \sin(p_{1,\mathrm{k}}) - \sin(p_{2,\mathrm{k}}). \end{cases} \tag{8}$$

As there might be many possible solutions for the Eq. 8, $p_{1,k}$ and $p_{2,k}$ are took in a way that they are nearby to $p_{1,k-1}$ and $p_{2,k-1}$ and raising or falling linearly. The frequency and situation offsets are then detected by a resolving a rectilinear regression allowing to the below equations:

$$\begin{cases} p_{1,\mathrm{k}} = (SpS)\,\omega_1 k + \phi_1, \\ p_{2,\mathrm{k}} = (SpS)\,\omega_2 k + \phi_2. \end{cases} \tag{9}$$

D. Preamble Detection of MA Receiver

A window with the span of the *Sync* preamble is always sliding on the obtained samples. Then each time the above *CFO* estimate algorithm is referred and they are wont to decode the next *LSFD* symbols of the packet where *LSFD* is the length of the *SFD* component. If the decoded *SFD* adjusts the guessed *SFD*, which is *XOR* of *SFD* of node *U* and node *V*, then the packet is detected and the remain of the symbols are decoded applying the similar parameters. In our propose, *SFDs* by nodes *U* and *V* are "1010 0110 1101 0110" and "1010 1010 0110 1011", severally, hence the *SFD* guessed in the relay is "0000 1100 1011 1101". Due to the presence of *CFO* and state offset, the constellation is altering from one symbol to another. The correct constellation for each obtained symbol is found applying the *i* and then applied for decoding and mapping, as following to the mapping function.

IV. THE EVALUATION OF PERFORMANCE

In our experiment, the real gain of *PNC* can be found in multi-hop transmissions, the similar execution is utilized for computing performance parameters in a Multi-hop Physical Layer Network Coding (*MPNC*). The core *MPNC* network blueprint applied for multi-hop experimentations is took from [6]. Then applying asynchronous tests the similar two hop performance parameters are computed for multi-hop *PNC* too. It is deserving referring that an exact computation of *RSS* or Channel State Information (*CSI*) is not demanded for the proposed algorithm to reach its most beneficial performance. The intention of the algorithm is to get nodes that are in one group around each other, so reaching exact Voronoi cells or the group that boundary nodes will bring together does not involve the last performance.

This is depicted in the evaluation whereas performance of path-loss channel and Rayleigh fading channel are really close to one another. The *GST* can be as little as an *ACK* time and there should be some guard length duration between pilot communications from group chiefs. The grouping can be started at every *GUP* time. It can also be activated by the *AP* if the arbitrarily chose headers effect in inadequate performance of network. Whenever network nodes are not uniformly spread, the *AP* can do the group chief choice non-randomly too, e.g. by choosing more or less of the nodes that suffer highest from contention as group chief. Including *M* in *BF* is something that is so soon being done in the IEEE standard draft [12]. Notifying group chief about their index can also be done applying a mapping scheme like to the one utilized for delivery traffic denotation recognized as *DTIM*. Our algorithm is also robust against collision from other *APs*. Since the *GSTs* are small and they could be carried sequentially with a gap of *SIFS*, any other *CSMA/CA* based station, e.g., other *APs*, cannot transfer anything during the grouping operation.

V. ANALYTICAL MODEL

To compare the performance of grouping schemes on hidden-terminal probability, here we set two metrics and apply them with the probability of having a hidden terminal in a group to depict the gains and costs of each grouping scheme. The 1st metric is the mean distance between nodes in a group, D_m, which is determined as:

$$D_m = \frac{\sum_i \sum_{j \neq i} d_{ij}}{(2^{n_m})} \, P_t, \forall_i and \; j\varepsilon \qquad group \; m \tag{10}$$

where n_m is the number of nodes in set m and d_{ij} is the length between nodes i and j.

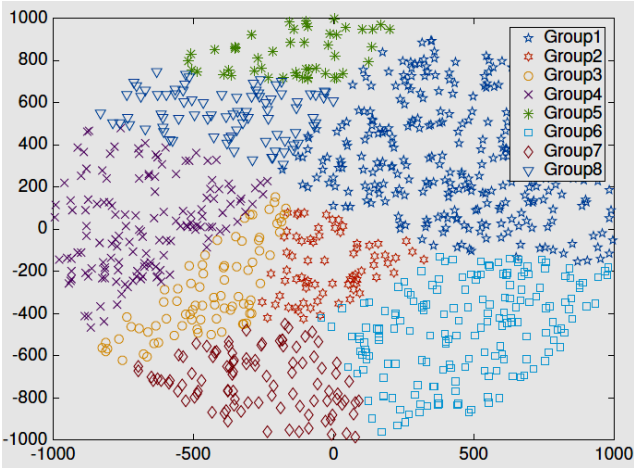

Fig. 2. A sample grouping depecting how nodes are classified position-wise applying RSS-based grouping.

The 2nd metric is the standard deviation of the amount of nodes in various groups which detects how evenly nodes are circulated within different groups.

$$\sigma = \sqrt{\frac{1}{G}\sum_{g=0}^{G-1}\left(n_g - \frac{N}{G}\right)^2} \tag{11}$$

where N defines the total number of nodes and G is the number of available groups. The following step is determining the chance of encountering the hidden terminal trouble for diverse schemes. The amount of group chief nodes in our suggested strategy is biased so their locations follow Binomial Point Process (*BPP*) and there are M of them in the whole coverage area. Thus, the chance that there are k group chiefs in an area of size B can be determined as:

$$\Pr[N(V) = k \mid N(U) = M] = \binom{M}{k}\left(\frac{V}{U}\right)^k \left(1 - \frac{V}{U}\right)^{M-k} \tag{12}$$

where $U = \pi R^2$ is total field of network. We applied D to mention the distance between one node and its nearest group chief. Every node will settle its closest group chief, hence for the *CDF* of D we have:

$$F_D(x) = 1 - \Pr[N(S(x)) = 0 \mid N(U) = M \qquad x \geq 0, \tag{13}$$

where $S(x)$ is the overlapping area between a circle focused at the studied node with radius x and the coverage region. Generally $S(x) \leq \pi x^2$ and the inequality happens for nodes secure to the coverage area's edge. We denote $F\hat{}(x)$ by:

$$F_D(x) = 1 - \Pr[N(\pi x^2) = 0 \mid N(U) = M \qquad 0 \leq x \leq R. \tag{14}$$

It is always fact that $F_D\hat{}(x) \geq F_D(x)$ for $0 \leq x \leq R$. Nevertheless, when M is large enough, which is generally the event in follow [13] the group size is hence tiny comparing with the entire network field that the variety between $F_D(x)$ and $F_D\hat{}(x)$ becomes insignificant. We apply the latter as an upper-bound of the real case.

$$\begin{aligned} F_D(x) \approx F_D(x) &= 1 - \Pr[N(\pi x^2) = 0 \mid N(U) = M \\ &= 1 - \binom{M}{0}\left(\frac{\pi x^2}{U}\right)^0 \left(1 - \frac{\pi x^2}{U}\right)^M \\ &= 1 - \left(1 - \frac{\pi x^2}{U}\right)^M \qquad 0 \leq x \leq R \end{aligned} \tag{15}$$

The validity of this estimate is then affirmed by simulation in preceding section. We can obtain *PDF* of D by choosing derivative of its *CDF*:

$$f_D(x) = \frac{2\pi M x}{U}\left(1 - \frac{\pi x^2}{U}\right)^{M-1} \qquad 0 \leq x \leq R \tag{16}$$

Applying this *PDF* we can acquire the chance of getting a hidden terminal when our RSS-based grouping pattern is applied

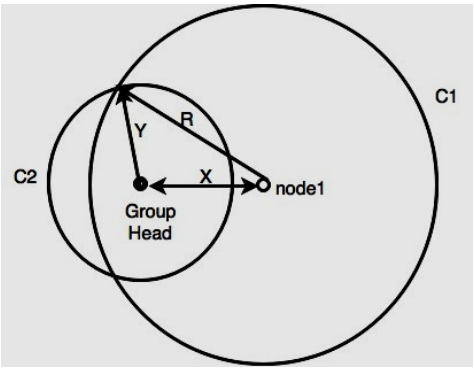

Fig. 3. Group chief in node-1 of Voronoi cell within 2 nodes.

Fig. 3 depicts a group chief and an arbitrary node mentioned node 1 in the linked group in distance X where X is the PDF in (16). The circle *C1* demonstrates the sensing series of node 1 and *C2* is a circle centered by the cluster chief on the radius Y which also comes the PDF in Eq. 16. The chance for node 2 which is Y outside from the cluster chief to be in the detection array of node 1 is the ratio of the function of *C2* inside *C1* to the perimeter of *C2*. Then, we can get the standard over the PDF of X and Y to obtain the probability that two nodes are in each other's sensing series.

$$\Pr_{sense} = \int_0^{\frac{U}{\pi}} \int_0^{\frac{U}{\pi}} \frac{g_1(x,y)}{2\pi y} fx(x) fY(y) dxdy \quad (17)$$

where Pr_{sense} is the probability that 2 nodes in the alike cluster are in each other's perception series, R_s is the sensing scope of a node,

$$g_1(x,y) = \begin{cases} 2\pi y & R_s \geq x+y \\ 2y \arccos\left(\frac{x^2+y^2-R_s^2}{2xy}\right) & R_s < x \mid +y \\ 0 & R_s < \mid x-y \mid \end{cases}, \quad (18)$$

and f_X (x) and f_Y (y) are the *PDF* of *X* and *Y* correspondingly. We can also obtain the corresponding chance for arbitrary grouping schemes. The chance density function for the length between 2 arbitrary nodes inside a circle on the radius *R* define in [14]:

$$f(r) = \frac{2r}{\pi}\left(\frac{2}{R^2}\arccos\left(\frac{r}{2R}\right) - \frac{r}{\pi R}\sqrt{1-\frac{r^2}{4R^2}}\right), 0 < r < 2R \quad (19)$$

In this case, for random grouping, the chance of that 2 nodes in the alike group are in each other's sensing region can be obtained as follows:

$$\Pr_{sense} = \int_0^{2R} g_2(r) f(r) dx, \quad (20)$$

where

$$g_2(r) = \begin{cases} 1 & r \leq R_s \\ 0 & r > R_s \end{cases} \quad (21)$$

These chances can then be computed by numerical methods.

VI. SIMULATION BASED PERFORMANCE RATING

The performance of diverse grouping schemes is measured using *MATLAB* and *NS*-2 [15]. MATLAB is applied for numerical computations and *NS-2* is applied for throughput simulations. The network coverage is presumed to be a circle with radius 1 km which is the case in sub 1GHz network bearing the entrance point at the focus. As noted in previous section, nodes are equivalently put in the coverage area with their number following a Poisson distribution with density 0.0019 node per square meter which effects in 6000 nodes in the network on the average. The amount of groups, *M*, was set in the range of 8 to 512. For each setting, the tests were repeated 20 times, and the mean was accepted.

If the *AP* the discovers position data of all the nodes, in a pure centralized answer where *AP* chooses the group for each node, the *k*-means algorithm can be applied to reach near-optimal groupings where the *k* value which presents the amount of clusters is equal to the amount of groups. So we can apply the performance with *k*-means grouping as a standard to check how considerably our *RSS*-based distributed grouping algorithm is functioning compared with the centralized benchmark. In Fig. 4 (a), the mean space within nodes in a group for the suggested scheme is always little than with the random grouping scheme and close to the *k*-means clustering algorithm. It is also observable that a large number of groups have a littler average length between nodes for all algorithms.

In Fig. 4(b), we can depict that the standard deviation of the amount of nodes in various groups is the cost that the RSS-based grouping algorithm gives for the gain of distributed solution. Groups with a large amount of users will suffer from high congestion chance and groups with a very little number of users might not full use their *RAW*. It is disclosed later utilizing *NS-2* simulations, that despite having some dense groups, the RSS-based grouping algorithm has improved operation than arbitrary groupings. This is since the hidden node trouble is a more severe trouble than uneven groups. A couple of hidden terminals can dramatically cut down the performance of the whole network.

Having more nodes that are all in the sensing range raises the competitor but has a less destructive result on the output than that because of hidden terminal. Accepting that all nodes have the similar sensing range, R_s, the chance of 2 random nodes in the comparable group be in their detection range versus R_s for a fixed number of groups is exposed in Fig. 5(a). The figure also presents that the estimate in Eq.15 not influence the solution very much.

As we can observe in the graphs, most beneficial performance is for the clustering using the *k*-means algorithm but the *RSS*-based grouping scheme also does very close to the *k*-means and very much better than the arbitrary grouping schemes. The same chance presuming Rayleigh fading channel among nodes is also depicted in Fig. 5 (a).

The performance with Rayleigh fading channels is disgraced for considering fast fading the fields concerned by groups are no longer Voronoi and the group chief with the highest perceived power is not basically the closest one. As depicted in the graphs the algorithm at rest executes well which defines that, the RSS estimation accuracy required is low, which outcomes in a small overhead.

On the simulation outcome coming analytical outcome, our assumption in preceding section is verified. The simulation and analytical outcome are nearer to each other as *M* raises. That is because, with a higher measure of *M*, the edge reach becomes more negligible. Fig. 5(b) depicts the chance does not alter with the number of groups for random grouping because nodes in the similar group can even be anyplace in the coverage region and their length till comes the same *PDF*.

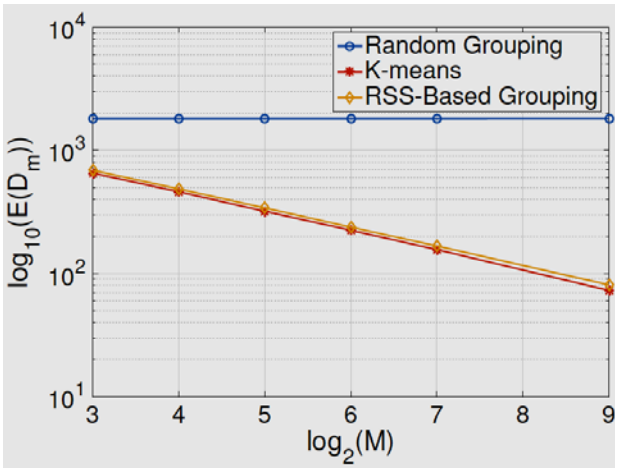

(a). Mean D_m over all groups

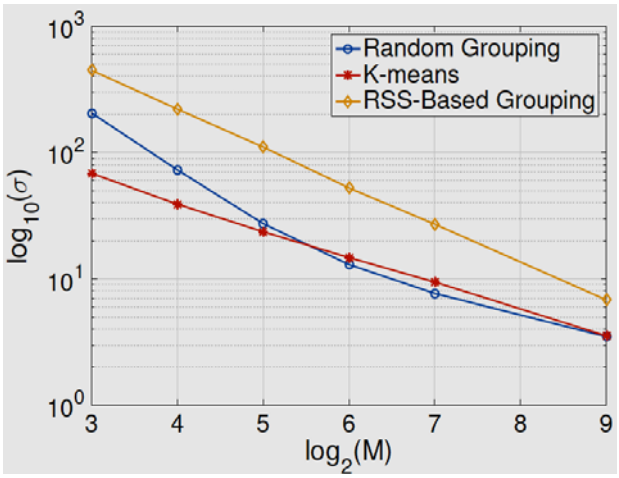

(b). The no. of nodes *SD* in different groups

Fig. 4. Grouping operation metrics

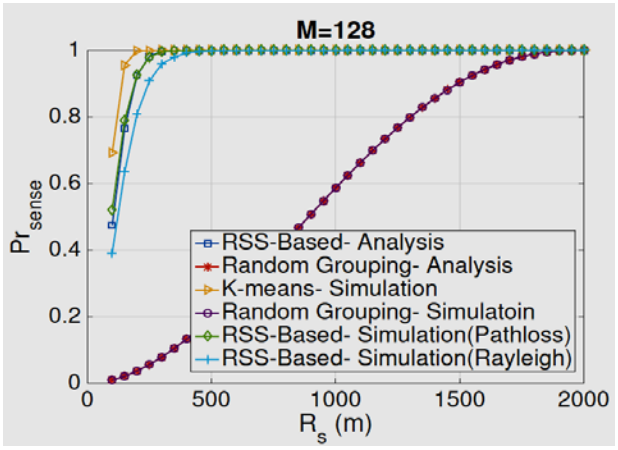

(a)

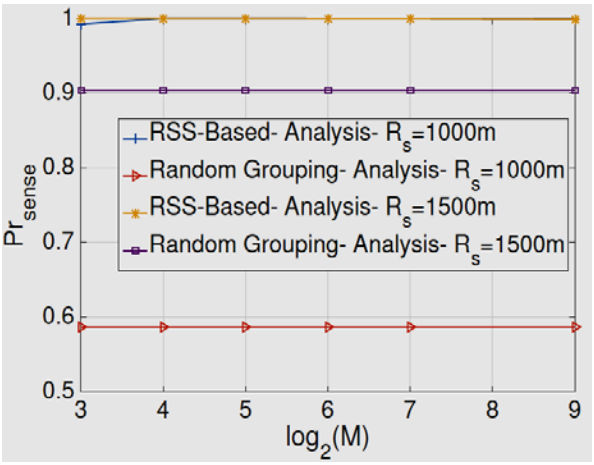

(b)

Fig. 5. Possibility of the sensing rate within 2 nodes,in a group.

Although case of the *RSS*-based grouping algorithm, a superior number of groups outcomes in a superior chance for group members to be in the sensing range of one another as it makes the Voronoi cells smaller. Fig. 6 depicts the output simulation result for dissimilar grouping schemes alongside with *k*-means clustering algorithm using *NS-2*. Table I presents the argument fixing for simulations applied in this section. Other common configuration e.g. *PHY* and *MAC* header are set according to the IEEE 802.11 standard [16]. The payload size is determined to be low considering the *IoT* purposes such as smart meter computation describing and all nodes are applying *RTS/CTS* mechanism[17]. Just the uplink traffic is viewed and a non-collided transmission is presumed to be successful which that entails the *PHY* layer *BER* is not considered [18].

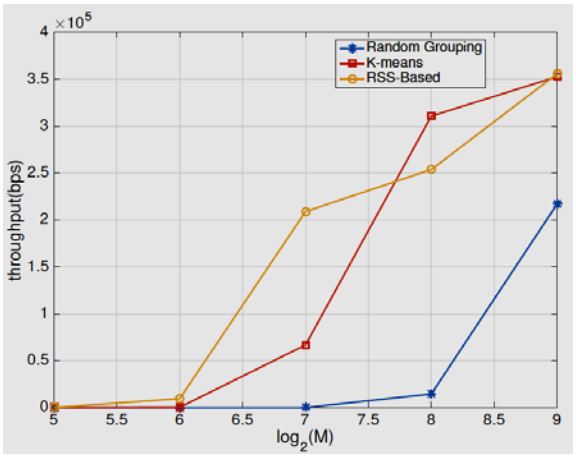

Fig. 6. Transmission uplink traffic

In Fig. 6, the output for random scheme is really low as the time for a single packet transmission is more largest back off window (1024 slots) and nearly any transmission would be interrupted when there are a couple of active nodes who are hidden terminals.

TABLE I. PARAMETER SETTING OF THROUGHPUT SIMULATION

Parameters	Value
Slot time	20 µS
SIFS	10 µS
Payload Size	64 bytes
Data Rate	1Mbps
Rs	1600
CW min	31
CW max	1023

Put differently, a node with a hidden terminal might just achievement in transmitting a packet to the AP without congestion. This scenario also illustrates the special cost that RSS-based grouping pays due to the higher variance of amount of nodes in each group. The output applying the commended RSS-based grouping is roughly that applying the centralized *K*-mean solution. Then again, random grouping has a lot worse operation because of the hidden terminal trouble even when the perception range is as high as 1600m. Mention that the theoretical sensing form without thinking the shadowing outcome may be much higher than the real sensing scope, so grouping looking at the location is significant to avoid hidden terminal and enhance network performance.

VII. CONCLUSION

In this research there are 2 technical wireless networking model supporting IoT that have the main focus for this paper. In single-hop transmission, overcrowded networks and IEEE *802.11aj* as a predicting standard for sensor networks are reviewed and the hidden terminal difficulty has been covered. An RSS-based grouping engineering has been suggested which will clusters users in RSS-based groups so nodes in the similar group can be near adequate that the chance of having a hidden terminal is really poor. The operation of RSS-based grouping has been then analyzed and tested to random and optimal grouping schemes applying analytical and simulation effect introducing diverse metrics. A special problem in future infrastructure based networks that can be resolved with RSS-based groups is small message size of almost sensing data exchanges, which will be minimizing channel effectiveness. In [19] illustrated that small packet size will minimize the overall throughput. RSS-based grouping schemes can operate clustering algorithms very easily where each group is a cluster and a cluster chief in each group can operate as a relay for other nodes. We intend to develop this application in our future work.

REFERENCES

[1] Alvandi, M., Mehmet-Ali, M. and Hayes, J.F., 2015. Delay optimization and cross-layer design in multihop wireless networks with network coding and successive interference cancelation. IEEE Journal on Selected Areas in Communications, 33(2), pp.295-308.

[2] Kong, L. and Liu, X., 2015, September. mzig: Enabling multi-packet reception in zigbee. In Proceedings of the 21st annual international conference on mobile computing and networking (pp. 552-565). ACM.

[3] Yang, H., Shin, W. and Lee, J., 2015, November. Degrees of freedom for K-user SISO interference channels with blind interference alignment. In 2015 49th Asilomar Conference on Signals, Systems and Computers (pp. 1097-1101). IEEE.

[4] Chen, B., Yenamandra, V. and Srinivasan, K., 2015, April. Interference alignment using shadow channel. In 2015 IEEE Conference on Computer Communications (INFOCOM) (pp. 2128-2136). IEEE.

[5] Jain, M., Choi, J.I., Kim, T., Bharadia, D., Seth, S., Srinivasan, K., Levis, P., Katti, S. and Sinha, P., 2011, September. Practical, real-time, full duplex wireless. In Proceedings of the 17th annual international conference on Mobile computing and networking (pp. 301-312). ACM.

[6] Zhang, H. and Cai, L., 2017. Bi-directional multi-hop wireless pipeline using physical-layer network coding. IEEE Transactions on Wireless Communications, 16(12), pp.7950-7965.

[7] Rahul, H., Hassanieh, H. and Katabi, D., 2011. SourceSync: a distributed wireless architecture for exploiting sender diversity. ACM SIGCOMM Computer Communication Review, 41(4), pp.171-182.

[8] Lu, L., Wang, T., Liew, S.C. and Zhang, S., 2013. Implementation of physical-layer network coding. Physical Communication, 6, pp.74-87.

[9] Lee, K. and Choi, H.H., 2018. Secure Analog Network Coding With Wireless Energy Harvesting Under Multiple Eavesdroppers. IEEE Access, 6, pp.76289-76301.

[10] Xiong, T., Zhang, J., Yao, J. and Lou, W., 2012, October. Symbol-level detection: A new approach to silencing hidden terminals. In 2012 20th IEEE International Conference on Network Protocols (ICNP) (pp. 1-10). IEEE.

[11] Patrick Ho Wang Fung, Sumei Sun, and Chin Keong Ho. Preamble design for carrier frequency offset estimation in two-way relays. In Signal Processing Advances in Wireless Communications (SPAWC), 2010 IEEE Eleventh Interna- tional Workshop on, pages 1–5. IEEE.

[12] IEEE 802 LAN/MAN Standards Committee. (2009). IEEE Standard for Information technology-Telecommunication and information exchange between systems-Local and metropolitan area networks-Specific requirements Part11: Wireless LAN Medium Access Control (MAC) and Physical Layer (PHY) Specifications Amendment1: Radio Resource Measurement of Wireless LANs.

[13] Zheng, L., Ni, M., Cai, L., Pan, J., Ghosh, C. and Doppler, K., 2014. Performance analysis of group-synchronized DCF for dense IEEE 802.11 networks. IEEE Transactions on Wireless Communications, 13(11), pp.6180-6192.

[14] Qureshi, K.N., Abdullah, A.H., Mirza, A. and Anwar, R.W., 2015. Geographical forwarding methods in vehicular ad hoc networks. International Journal of Electrical and Computer Engineering, 5(6).

[15] Bi, S., Ho, C.K. and Zhang, R., 2015. Wireless powered communication: Opportunities and challenges. IEEE Communications Magazine, 53(4), pp.117-125.

[16] Wireless LAN medium access control (MAC) and physical layer (PHY) specifications amendment 8: IEEE 802.11 wireless network management, September 2011.

[17] Islam, C.S., 2015, June. A novel idea of coupling licensed and unlicensed users using distributed harmonizing algorithm (DHL) in cognitive radio networks (CRNs). In 2015 International Conference on Informatics, Electronics & Vision (ICIEV) (pp. 1-6). IEEE.

[18] Islam, C.S., 2015, December. Minimizing the interference leakage using a novel IA algorithm to provide perfect alignment solutions. In 2015 18th International Conference on Computer and Information Technology (ICCIT) (pp. 435-439). IEEE.

[19] Chen, Z., Fu, D., Gao, Y., & Hei, X.. Performance evaluation for WiFi DCF networks from theory to testbed. In 2017 IEEE International Symposium on Parallel and Distributed Processing with Applications and 2017 IEEE International Conference on Ubiquitous Computing and Communications (ISPA/IUCC) (pp. 1364-1371). IEEE.